


Nonlinear Optical Pulses in Media with Asymmetric Gain

S. K. Turitsyn¹, A. E. Bednyakova², and E. V. Podivilov³

¹*Aston Institute of Photonic Technologies, Aston University, Birmingham B4 7ET, United Kingdom*

²*Novosibirsk State University, Novosibirsk 630090, Russia*

³*Institute of Automation and Electrometry, SB RAS, Novosibirsk 630090, Russia*

 (Received 27 February 2023; accepted 5 September 2023; published 12 October 2023)

A generic novel model governing optical pulse propagation in a nonlinear dispersive amplifying medium with asymmetric (linear spectral slope) gain is introduced. We examine the properties of asymmetric optical pulses formed in such gain-skewed media, both theoretically and numerically. We derive a dissipative optical modification of the classical shallow water equations that highlights an analogy between this phenomenon and hydrodynamic wave breaking. These findings provide insight into the nature of asymmetric optical pulses capable of accumulating large nonlinear phase without wave breaking, a crucial aspect in the design of nonlinear fiber amplifiers.

DOI: [10.1103/PhysRevLett.131.153802](https://doi.org/10.1103/PhysRevLett.131.153802)

In many physical and engineering problems dealing with optical amplification a frequency dependence of the gain (that usually is broader compared to the considered signal bandwidth) is assumed to be symmetric and is often approximated by the Lorentzian spectral shape [1,2]. This is, typically, a justified assumption in the spectral region near the peak of the gain curve. There are, however, relatively fewer explored possibilities to use edges of the gain profile that is not symmetric. Here, we examine the impact of asymmetry in the spectral gain shape on formation and evolution of optical pulses at the carrier frequency ω_0 in an amplifying nonlinear dispersive medium, considering the simplest linear asymmetric gain profile, that in the frequency domain reads

$$g(\omega) = g_0 - g_1(\omega - \omega_0).$$

The slope of the gain asymmetry can be both positive or negative depending on the sign of g_1 . Higher-order terms can be easily included, however, we focus here on the impact of the most general first-order approximation of the gain asymmetry. Of course, we assume that at larger deviations from ω_0 linear spectral dependence will be changed and gain will not grow to infinity making the problem ill posed. Note that propagation of the light field affected both by gain and loss can be of interest for studies of optical systems with parity-time symmetry [3].

In the recent works of the Cornell group [4] a new type of asymmetric nonlinear pulse propagation was demonstrated, distinguished by the presence of a dynamically evolving gain spectrum. Nonlinear spectral broadening of the pulse led to its reshaping due to absorption and amplification. The dynamic change of the gain and spectral broadening led to quasistable regimes where pulse was partially propagating at the edge of the material gain curve. We anticipate that our analysis of a much more simple “minimal” model will provide useful insight into characteristics of nonlinear pulse propagation in a medium with spectrally asymmetric amplification, beyond standard parabolic gain curve approximations.

Consider propagation of an envelope of the optical field $\psi(z, t)$ down the amplifying dispersive optical medium with Kerr nonlinearity within the framework of the one-dimensional generalized nonlinear Schrödinger equation (NLSE) with asymmetric gain.

$$i \frac{\partial \Psi}{\partial z} - \frac{\beta_2}{2} \frac{\partial^2 \Psi}{\partial t^2} + \gamma |\psi|^2 \psi = i g_0 \Psi + g_1 \frac{\partial \Psi}{\partial t}. \quad (1)$$

Here, β_2 is the group velocity dispersion, γ is the nonlinear Kerr coefficient, z is a propagation spatial coordinate, t is a standard retarded time [2], and g_0 and g_1 define a gain profile. Equation (1) is well studied for the case $g_1 = 0$, when it governs parabolic pulse formation in the central energy-containing part (see, e.g., [5–10] and references therein). A self-similar parabolic pulse is an approximate wave breaking free solution of Eq. (1) (with $g_1 = 0$). We would like to reiterate that formally this equation is ill posed due to the infinite growth of the gain at large frequencies. However, we prefer here not to introduce any formal mathematical regularization that will change generality of the model, but instead stress that the equation

Published by the American Physical Society under the terms of the Creative Commons Attribution 4.0 International license. Further distribution of this work must maintain attribution to the author(s) and the published article's title, journal citation, and DOI.

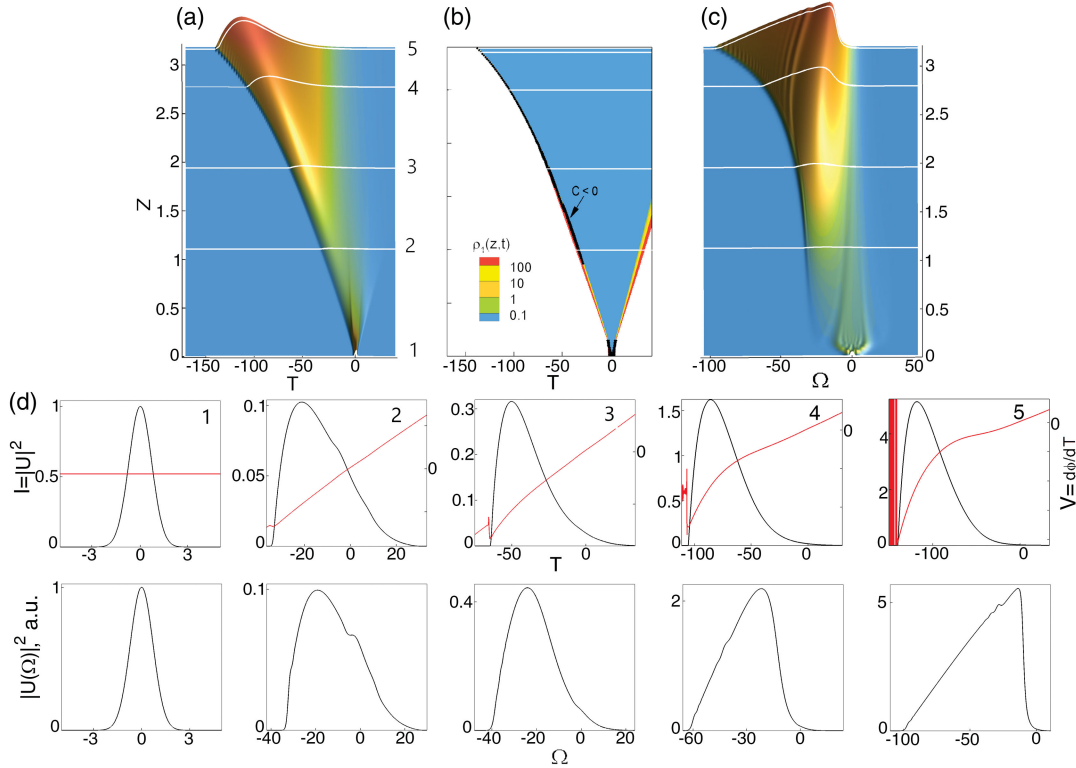


FIG. 1. Formation of asymmetric nonlinear pulses without OWB (at the propagation distances $Z \leq 3$): (a) and (c) Show 3D evolution of pulse intensity and power spectral density, respectively. (b) Shows in the plane (Z, T) a function $\rho_1(Z, T) = 0.5\epsilon|U(Z, T)|^{-3}(\partial^2|U(Z, T)|/\partial T^2)$ that defines applicability of the “quasiclassical” approximation [Eqs. (3) and (4)]. The middle row shows pulse intensity (black lines) and instantaneous frequency at Z_k corresponding to the horizontal lines marked with the index k ($k = 1, 2, 3, 4, 5$) in the upper row. The bottom row shows the power spectral density at Z_k . Here, $\epsilon = 0.004$, $\delta = 0.045$.

is valid only in the area (in the frequency domain) around ω_0 where gain can be approximated by a straight line and should not be used beyond this spectral region.

In what follows, we consider only the case $g_0 = 0$, because solutions of Eq. (1) $A(z, t)$ with $g_0 = 0$ and $\Psi(z, t)$ with $g_0 \neq 0$ can be expressed by each other using the transform $\Psi(z, t) = A(z, t - \beta_2 g_0 z / g_1) \exp(-i g_0 t / g_1 + i 0.5 \beta_2 g_0^2 z / g_1^2)$, that has a transparent physical meaning of the effective central frequency shift by the Galilean transformation. In what follows we will use a retarded time $t_r = t - \beta_2 g_0 z / g_1$ for $A(z, t_r)$ and will skip index r in notation. Below, similar to [2] we will use variable ω for the detuning around the central frequency ω_0 . Equation (1) (with $g_0 = 0$) has two conserved integrals, energy E and the Hamiltonian H :

$$E = \int |A(z, t)|^2 \exp\left[\frac{2g_1 t}{\beta_2}\right] dt,$$

$$2H = \int (\beta_2 |A_t|^2 + 2g_1^2 |A|^2 / \beta_2 + \gamma |A|^4) \exp\left[\frac{2g_1 t}{\beta_2}\right] dt.$$

The simple way to prove this is to make a transformation $A(z, t) = B(z, t) \exp[-g_1 t / \beta_2]$ with the equation for the field B being conservative.

In this Letter, we consider the evolution of the initial Gaussian pulse $A(t, z = 0) = \sqrt{P_0} \exp[-t^2 / (2T_0^2)]$ in Eq. (1). In the linear case ($\gamma = 0$) pulse experiences amplification combined with the conventional broadening, while continuously accelerating: position of the pulse $t_p(z)$ peak power is changing following the parabolic trajectory: $t_p(z) = -\beta_2 g_1 z^2 / T_0^2$. The direction of the drift is defined by the sign of the product of dispersion and gain slope parameter $\beta_2 g_1$. Gain slope leads to the continuous shift of the position of the pulse spectral power maximum in the frequency domain: $\omega_p(z) = -g_1 z / T_0^2$. In the linear medium, evolution of the considered initial pulse preserves its symmetric Gaussian shape both in time and frequency domains; see Supplemental Material [11] for details.

In the nonlinear regime, however, the initially symmetric wave form evolves into asymmetric pulse. It is convenient to rewrite Eq. (1) in the normalized form with two dimensionless parameters ϵ and δ :

$$i \frac{\partial U}{\partial Z} - \frac{1}{2} \frac{\partial^2 U}{\partial T^2} + \frac{1}{\epsilon} |U|^2 U = \delta \frac{\partial U}{\partial T}. \quad (2)$$

Here, $A(z, t) = \sqrt{P_0} U(Z, T)$, $T = t / T_0$ ($\Omega = \omega T_0$), $U(z, T) = \int U(z, \Omega) \exp(-i \Omega T) d\Omega$, $Z = z / L_{\text{dis}}$, with

$L_{\text{dis}} = T_0^2/|\beta_2|$. We consider the so-called normal dispersion medium with $\beta_2 > 0$. Parameters $\epsilon = |\beta_2|/(\gamma P_0 T_0^2) = L_{\text{NL}}/L_{\text{dis}}$ (see, e.g., [2]) and $\delta = g_1 T_0/|\beta_2|$ define the pulse evolution. Parameter ϵ characterizes the interplay between dispersive and nonlinear effects and is small in highly nonlinear regimes considered here.

Similar to amplification with constant gain [5,6], depending on the initial power and temporal width [that correspond to different points in the (ϵ, δ) plane], Gaussian pulse evolution in Eq. (2) can lead to regimes with (i) the optical wave breaking (OWB) [15,16] defined as an overtaking of different parts of the pulse, and nonlinear generation of new frequencies during overtaking, or (ii) without wave breaking (up to a certain distance), for details, see Supplemental Material [11]. As we will show below, the type of the nonlinear evolution is determined by an interplay between the so-called “quantum pressure” term in Eq. (2) (for details, see, e.g., [17,18]): $(1/2|U|)[(\partial^2|U|)/\partial T^2] = \rho_1|U|^2/\epsilon$ and the pulse chirp introduced as $C = -(\partial^2/\partial T^2) \arg(U)$, with the parameter ρ_1 [a ratio between the “quantum pressure” and the nonlinear term $|U|^2/\epsilon$ in Eq. (2)] playing an important role in the defining conditions of a wave breaking.

Propagation of the initial Gaussian with the parameters $\epsilon = 0.004$ ($L_{\text{dis}}/L_{\text{NL}} = 250$), $\delta = 0.045$ (corresponding to point “1”, in the map described in Supplemental Material [11]) leading to the formation of the asymmetric pulse is shown in Fig. 1. The upper row shows 3D dynamics of (a) $I(Z, T) = |U(Z, T)|^2$ and (c) $|U(Z, \Omega)|^2$. The middle figure in the upper row depicts in the plane (Z, T) a function $\rho_1(Z, T) = 0.5\epsilon I^{-3/2}(\partial^2\sqrt{I}/\partial T^2)$. In the area where $\rho_1 < 0.1$ one can apply the Whitham quasiclassical approach [17,19], to derive simplified model Eqs. (3) and (4) below. The middle row in Fig. 1 shows at the points $Z = Z_k$ (corresponding to the lines marked with the index k in the upper row figures) intensity of the pulse $I(Z_k, T)$ ($k = 1, 2, 3, 4, 5$) (black lines) and an instantaneous frequency (red lines). The bottom row shows $|U(Z_k, \Omega)|^2$ at the same distances Z_k . It is seen that the energy-containing part of the pulse is moving to the negative T experiencing amplification and shape change. The pulse trailing edge stays in the lossy area, see spectrograms in Fig. S2 in Supplemental Material [11].

Figure 2 depicts in the linear (left) and logarithmic (right) scales three characteristic regions across the pulse at the point $Z = Z_3$. Here, we change the scales to zoom the pulse structure. In the zone I, at the leading edge, pulse shape is close to parabola allowing to avoid wave breaking, similar to the medium with constant gain [7], in the zone III (both on the left and right), pulse has exponential asymptotic determined by the linearized equation, similar to [6,9]. Zone II corresponds to the energy containing, nonparabolic part of the asymmetric pulse wave form.

For high pulse powers, when the characteristic nonlinear length L_{NL} is much smaller than the dispersive length

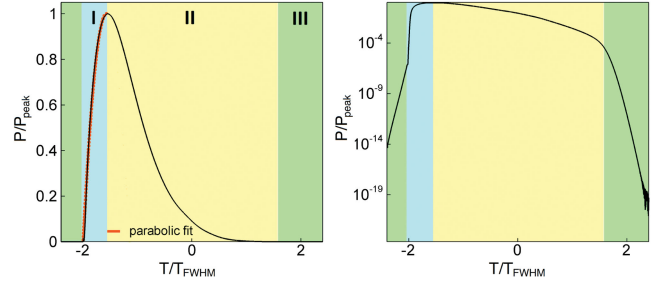


FIG. 2. Rescaled details of the temporal shape of a pulse from Figs. 1(d)–3. Here, $|U(Z_3, T)|^2 / \max_T(|U(Z_3, T)|^2)$ is shown in the normal (left figure) and logarithmic (right figure) scales. T_{FWHM} is the pulse full width at half maximum at $Z = Z_3$.

$L_{\text{dis}}: L_{\text{NL}}/L_{\text{dis}} = \epsilon \ll 1$, it is customary to consider the so-called quasiclassical limit (see, e.g., [17–22] and references therein), when we can neglect time variations of the field amplitude compared to phase time changes.

After applying the well-known Madelung transformation $I = |U|^2$ and $V = -(\partial/\partial T) \arg(U)$, [17,19] we get a reduced model for I and V , that is a modification of the one-dimensional shallow water equations [17–19,23,24]:

$$\frac{\partial I}{\partial Z} = -\frac{\partial IV}{\partial T} - 2\delta IV, \quad (3)$$

$$\frac{\partial V}{\partial Z} = -\frac{\partial V^2}{\partial T} - \frac{1}{\epsilon} \frac{\partial I}{\partial T}, \quad (4)$$

Here, we neglect the time derivatives $S_1 = (1/2\sqrt{I})(\partial^2\sqrt{I}/\partial T^2)$ and $S_2 = (\delta/2I)(\partial I/\partial T)$ compared to I/ϵ (see Supplemental Material [11] for details). Evolution of the asymmetric pulse can be described by the modified shallow water equations (3) and (4) ($\rho_1 = \epsilon S_1/I$ and $\rho_2 = \epsilon S_2/I$ are both small compared to unity) in the blue area shown in Fig. 1(b). Evidently, at the pulse edges this simplified description is not valid [9]. This is a direct analogy with self-similar parabolic solution [5,6,9,16] described by the NLSE or NLSE with the spectrally flat constant gain.

Without the second term in the right-hand side of Eq. (3), Eqs. (3) and (4) have the symmetry: $I(-T, Z) = I(T, Z)$, $V(-T, Z) = -V(T, Z)$ and any initially symmetric distribution holds this property during the propagation. However, this term breaks the symmetry, leading to the transformation of even a symmetric initial distribution into a skewed one during the evolution in Z . Note that in the shallow water equations asymmetry caused by a sloping beach (mathematically different from our case) was studied in [25].

The wave breaking (gradient catastrophe) phenomenon in Eq. (4) is determined by the sign of the chirp. When chirp becomes negative at some point: $\partial V/\partial T < 0$, wave breaking that manifests itself through the formation of a vertical jump in the amplitude in the field V is inevitable [in the

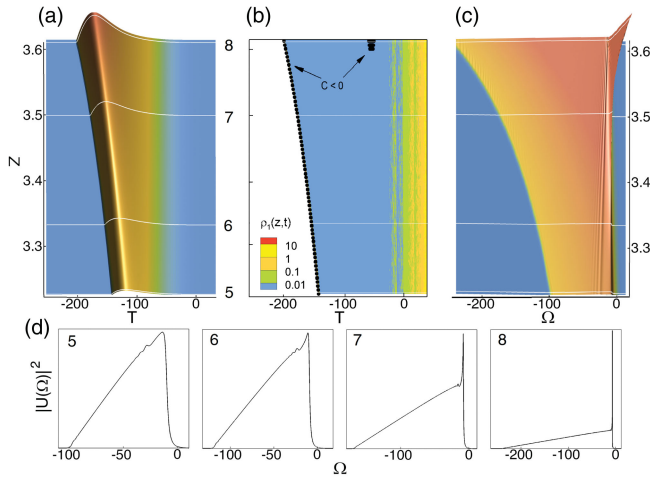


FIG. 3. Continued Fig. 1: (a) and (c) Show 3D evolution of pulse intensity and power spectral density, respectively. Middle figure in the upper row shows a function $\rho_1(Z, T)$. The bottom row shows the power spectral density at the points Z_k corresponding to the horizontal lines marked with the index k in the upper row figures. Here, $\epsilon = 0.004$, $\delta = 0.045$.

framework of Eqs. (3) and (4) [19]. A negative chirp can only occur due to nonlinearity (see, e.g., [2] for details). The self-phase-modulation (SMP)-induced frequency chirp is negative for a convex function with $\partial^2 I / \partial T^2 > 0$ and positive for a concave function with $\partial^2 I / \partial T^2 < 0$. That is why for a parabolic pulse shape ($\partial^2 I / \partial T^2 < 0$) SMP-induced frequency chirp is positive and no wave breaking occurs.

While Eqs. (3) and (4) are useful for understanding of the wave breaking, it is important to examine their applicability. Figure 1(b) shows the parameter $\rho_1(Z, T)$ across the pulse. The black color indicates an area of negative chirp where the process of wave breaking is triggered. It is seen that the chirp is negative at the leading edge of the pulse, where ρ_1 is not small anymore. Thus, Eqs. (3) and (4) are invalid in the area of negative chirp. Terms neglected in Eqs. (3) and (4), such as the temporal derivative S_1 , prevent wave breaking in the full model given by Supplemental Material, Eqs. (S3) and (S4) (see Ref. [11] for details). The change of sign of the chirp at the leading edge of the pulse from positive to negative that can be seen in Fig. 1(d) (third figure) is similar to the parabolic pulse formation in the medium with constant, spectrally flat gain [5,6,8], where stabilization is observed at both edges of the pulse. However, the considered asymmetric pulse features different dynamics at the leading and trailing edges.

Namely, while the leading edge is “wave breaking free” due to the parabolic shape, a buildup of the SMP-induced negative chirp at the trailing edge of the asymmetric pulse leads to the development of a wave breaking, with a formation of high spectral peak in the vicinity of a zero frequency, as shown in Fig. 3. Figure 3 continues Fig. 1 (all parameters are the same) showing further propagation of the asymmetric pulse, after it is formed. It is seen that at the distance Z around 3.6 chirp becomes negative in the area

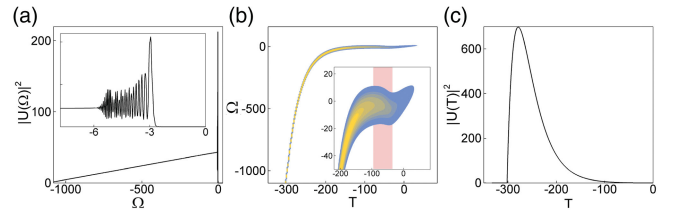


FIG. 4. Details of the spectral peak and oscillations (a), spectrogram (b), and temporal profile (c) of the asymmetric pulse shown in Fig. 3 at the start of the wave breaking at the trailing edge at $Z = 3.8$. Insets: close-up of the spectrum (a) and spectrogram (b) in the vicinity of $\Omega = 0$. The yellow (blue) color corresponds to the high (low) intensity.

where ρ_1 is small [Fig. 3(b)] and term with S_1 cannot stop wave breaking featuring initially the steepening of the spectrum depicted in Fig. 3(d). Figure 4(b) shows a nonmonotonic time-frequency dependence (negative chirp) and start of the corresponding spectral oscillations at the trailing (low power) edge of the pulse. Details of this effect will be discussed elsewhere.

In more accurate models, the gain is bandwidth limited, and its slope is linear only within a certain range of frequencies. Additionally, amplification typically becomes saturated at some level. While the inclusion of these physical effects makes the master model less generic, they combine to stabilize the propagation of nonlinear asymmetric pulses, preventing wave breaking. Figure S4 in Supplemental Material [11] shows that an asymmetric nonlinear pulse can propagate without wave breaking, adjusting its spectral and temporal shape to the gain profile, similar to [4]. Details of the numerical modeling in this case are provided in Supplemental Material [11].

In conclusion, a new (minimal) model describing optical pulse propagation in a nonlinear dispersive amplifying medium with a gain with linear spectral slope was introduced. An analogy with the hydrodynamic shallow water equations model is discussed. It is shown that negative chirp plays the key role in wave breaking and formation of a characteristic spectral optical shock waves in this model system. Observed asymmetric optical pulses capable to accumulate up to certain distance a large nonlinear phase without wave breaking might be interesting for various applications in high power systems.

The work of A. B. was supported by the Russian Science Foundation (Grant No. 17-72-30006). S. K. T. acknowledges support by the EU project HALT and the Isaac Newton Institute for Mathematical Sciences, Cambridge within the programme HYD2.

- [1] A. E. Siegman, *Lasers* (University Science Books, Mill Valley, California, 1986).
- [2] G. Agrawal, *Nonlinear Fiber Optics* (Academic Press, New York, 2012), Chap. 2.

- [3] C. E. Ruter, K. G. Makris, R. El-Ganainy, D. Christodoulides, M. Segev, and D. Kip, *Nat. Phys.* **6**, 192 (2010).
- [4] P. Sidorenko, W. Fu, and F. Wise, *Optica* **6**, 1328 (2019).
- [5] M. E. Fermann, V. I. Kruglov, B. C. Thomsen, J. M. Dudley, and J. D. Harvey, *Phys. Rev. Lett.* **84**, 6010 (2000).
- [6] V. I. Kruglov, A. C. Peacock, J. D. Harvey, and J. M. Dudley, *J. Opt. Soc. Am. B* **19**, 461 (2002).
- [7] J. M. Dudley, C. Finot, D. J. Richardson, and G. Millot, *Nat. Phys.* **3**, 597 (2007).
- [8] F. O. Ilday, J. R. Buckley, W. G. Clark, and F. W. Wise, *Phys. Rev. Lett.* **92**, 213902 (2004).
- [9] S. Boscolo, S. K. Turitsyn, V. Y. Novokshenov, and J. H. B. Nijhof, *Theor. Math. Phys.* **133**, 1647 (2002).
- [10] C. Finot, F. Parmigiani, P. Petropoulos, and D. J. Richardson, *Opt. Express* **14**, 3161 (2006).
- [11] See Supplemental Material at <http://link.aps.org/supplemental/10.1103/PhysRevLett.131.153802>, which includes Refs. [12–14] for detailed analysis of wave breaking and derivation of basic equations.
- [12] E. Madelung, *Z. Phys.* **40**, 322 (1927).
- [13] A. Peacock, R. Kruhlak, J. Harvey, and J. Dudley, *Opt. Commun.* **206**, 171 (2002).
- [14] D. Anderson, M. Desaix, M. Lisak, and M. L. Quiroga-Teixeiro, *J. Opt. Soc. Am. B* **9**, 1358 (1992).
- [15] W. J. Tomlinson, R. H. Stolen, and A. M. Johnson, *Opt. Lett.* **10**, 457 (1985).
- [16] D. Anderson, M. Desaix, M. Karlsson, M. Lisak, and M. Quiroga-Teixeiro, *J. Opt. Soc. Am. B* **10**, 1185 (1993).
- [17] G. A. El and M. Hoefler, *Physica (Amsterdam)* **333D**, 11 (2016).
- [18] G. Biondini, G. El, M. Hoefler, and P. Miller, *Physica (Amsterdam)* **333D**, 1 (2016).
- [19] G. B. Whitham, *Linear and Nonlinear Waves*, Pure and Applied Mathematics (Wiley, New York, 2011).
- [20] G. A. El, R. H. J. Grimshaw, and M. V. Pavlov, *Stud. Appl. Math.* **106**, 157 (2001).
- [21] G. Xu, J. Garnier, D. Faccio, S. Trillo, and A. Picozzi, *Physica (Amsterdam)* **333D**, 310 (2016).
- [22] G. Xu, M. Conforti, A. Kudlinski, A. Mussot, and S. Trillo, *Phys. Rev. Lett.* **118**, 254101 (2017).
- [23] A. Bendahmane, G. Xu, M. Conforti, A. Kudlinski, A. Mussot, and S. Trillo, *Nat. Commun.* **13** (2022).
- [24] S. Wabnitz, *J. Opt.* **15**, 064002 (2013).
- [25] G. F. Carrier and H. P. Greenspan, *J. Fluid Mech.* **4**, 97 (1958).